The Selective Chlorination of Iron from Ilmenite Ore by CO-Cl_2 Mixtures: Part I. Intrinsic Kinetics

K.I. RHEE and H.Y. SOHN

The intrinsic kinetics of the selective chlorination of iron from ilmenite ore using carbon monoxide as the reducing agent were studied in a shallow fluidized bed. Experiments on the effects of chlorination temperature, carbon monoxide and chlorine gas partial pressures, and particle size were conducted in the absence of mass- and heat-transfer influences. Results indicate that the kinetics in the temperature range 923 to 1123 K are represented by the following pore-blocking rate law:

$$\lambda\left[\exp\left(\frac{X_{Fe}}{\lambda}\right)-1\right]=33.7\exp\left(-\frac{E}{RT}\right)p_{CO}^{0.52}p_{Cl_2}^{0.32}t$$

where E is 37.2 kJ/mol and p and t are in atm (=101.3 kPa) and minutes, respectively. The partial pressure of carbon monoxide was found to affect the chlorination rate more strongly than that of chlorine. A reaction mechanism in which iron in ilmenite reacts with chlorine before the liberated oxygen is removed by carbon monoxide is proposed.

I. INTRODUCTION

TITANIUM has found increased use in aerospace and commercial applications, because it has an attractive combination of properties, such as excellent strength-to-weight ratio and high corrosion and erosion resistances.[1,2] Further, the demand for titanium dioxide, which is the most consumed of all the forms of titanium, is quickly growing in the paper and plastics industries, as well as in pigment industries.[3] High purity titanium metal and titanium dioxide are produced from the intermediate titanium tetrachloride which is obtained by the chlorination of a high-grade titanium ore, mainly rutile. However, deposits of rutile occur in a limited number of places, such as Australia, Sri Lanka, South Africa, India, and Sierra Leone;[4] we are experiencing a shortage, and it is becoming more expensive to mine. Therefore, other abundant low-grade titanium minerals, such as ilmenite ($FeTiO_3$), arizonite ($Fe_2O_3 \cdot nTiO_2 \cdot mH_2O$), leucoxene ($Fe_2O_3 \cdot nTiO_2$), perovskite ($CaTiO_3$), and titaniferous magnetite, must be utilized as substitutes for rutile.

Due to the high content of impurities in these minerals, especially iron, it is necessary to upgrade them to obtain synthetic rutile which is acceptable as a feedstock for chlorination. A number of processes[5–12] have been proposed for the removal of iron from low-grade titanium ore, such as chlorination by various agents with or without pretreatment, smelting followed by sulfation and hydrochloric acid leaching, hydrogen reduction followed by ferric salt leaching, high temperature/high pressure leaching with sulfuric acid in the presence of a reducing agent, and solid-state reduction followed by chemical or physical separation.

Among these processes, the direct chlorination has a significant advantage in that it can be done with conventional chlorination equipment and requires no pretreatment, such as roasting or slagging. However, some operational difficulties are associated with this process due to the defluidization and clogging caused by high boiling point metal chlorides produced during chlorination. Nonetheless, these difficulties can be removed by the control of temperature, amount of reducing agent, and the partial pressure of chlorine.

Usually, direct chlorination can be accomplished in two ways: One is the chlorination of both iron and titanium, forming volatile chlorides which are subsequently separated; and the other is the selective chlorination of iron in the ore, leaving a titanium oxide-rich residue. The selective chlorination also has the advantages of increasing the efficiency of chlorine consumption and requiring lower energy. In addition, iron removal from ilmenite and titaniferous ore results in increased porosity and surface area; thus, the reactivity of the treated material is generally high. Despite a number of investigations[5,6,13–15] on the direct chlorination of ilmenite, basic kinetics of the chlorination have not been elucidated.

In the present study, the kinetics of the selective chlorination of iron from ilmenite ore were determined in a shallow fluidized bed to eliminate mass- and heat-transfer effects and to prevent side reactions of the chlorides involved. It is noted that this paper is not concerned with the simulation of a fluidized-bed chlorination process but rather reports on the chemical kinetics of the chlorination reaction. Experiments were conducted to determine the effects of chlorination temperature, chlorine and carbon monoxide partial pressures, and particle size. Additionally, the effect of partial pressure of ferric chloride was investigated by adding vaporized ferric chloride to reactant gases.

In Part II of this paper,[16] mathematical modeling of the selective chlorination of ilmenite ore by CO-Cl_2 mixtures in a deep fluidized bed will be presented. The

K.I. RHEE, formerly Graduate Student at the Department of Metallurgical Engineering, University of Utah, is Head of Rare Metals Research Department, Korea Institute of Energy and Resources, Daejeon, Korea. H.Y. SOHN, Professor, is with the Department of Metallurgical Engineering, University of Utah, Salt Lake City, UT 84112-1183.

Manuscript submitted September 1, 1988.

kinetics of the selective chlorination using carbon as the reductant will be described in a subsequent article.[17]

II. EXPERIMENT

A. *Sample Preparation*

The ilmenite ore used in this experiment was a rock-type Quebec product purchased from Ward Mineral Co., Rochester, NY. This ore was crushed, ground, and classified into various mesh sizes, from 50 to 170 mesh. Each representative sample was subjected to analysis. A weighed sample was fused with lithium metaborate ($LiBO_2$) at 1223 K and then dissolved in a 0.5 N HCl solution. The resulting solution was analyzed by a direct current plasma (DCP) spectrometer. Although this analysis gives total iron in the ilmenite ore, the amount of ferrous and ferric can be calculated from the assumption that the ferrous exists only in the form of $FeTiO_3$. This is also confirmed by the titration analysis ($Fe^{2+} + Ce^{4+} = Fe^{3+} + Ce^{3+}$)[18] which was done by the Korea Institute of Energy and Resources. The results of this analysis are shown in Table I.

A predominant phase of ilmenite and minor phases of hematite and enstatite were identified by X-ray diffraction, as seen in Table II.

B. *Experimental Apparatus and Procedure*

A schematic diagram of the experimental apparatus is shown in Figure 1. The fluidized bed reactor consisted of a quartz tube measuring 2.5 cm in diameter and 33 cm in length and an enlargement section measuring 5 cm in diameter and 17 cm in length. This reactor was externally heated in a KANTHAL* resistance furnace. A fritted quartz disc was used as the gas distributor through which preheated gas was introduced. A CHROMEL-ALUMEL* thermocouple immersed in the bed was used to measure the temperature during the reaction. The connecting tube was wrapped with heating tape and maintained at 623 K to avoid the condensation of iron chloride.

*KANTHAL is a trademark of Kanthal Corporation, Bethel, CT.

*CHROMEL-ALUMEL is a trademark of Hoskins Manufacturing Company, Hamburg, MI.

A weighed amount of ilmenite was charged into the preheated reactor, while a flow of N_2 was maintained at 0.6 l/min (298 K and 86.1 kPa). When the temperature reached the desired value, the nitrogen flow was discontinued, and a predetermined gas mixture was passed through the gas distributor for a specified period of time. At the end of each run, ore residue was collected from the reactor, weighed, and analyzed for Ti and Fe by the DCP spectrometer.

Table I. Chemical Composition of Ilmenite Ore in Different Particle Size Fractions

Size Component	50/70 Mesh	70/100 Mesh	100/140 Mesh	140/170 Mesh
TiO_2	36.7	38.1	37.0	38.0
FeO	33.2	34.2	33.3	34.1
Fe_2O_3	19.0	17.1	19.6	18.1
SiO_2	4.26	4.43	4.02	4.45
MgO	3.32	3.08	3.13	3.10
CaO	0.45	0.60	0.71	0.62

Table II. X-Ray Diffraction Analysis of Ilmenite Ore

Mineral	Ilmenite Ore
Ilmenite ($FeTiO_3$)	major
Hematite (Fe_2O_3)	minor
Magnetite (Fe_3O_4)	—
Enstatite ($MgSiO_3$)	minor
Quartz (SiO_2)	—
Unidentified	—

III. RESULTS AND DISCUSSION

A. *Selectivity of Iron Chlorination*

An equilibrium diagram presenting the predominance areas of Fe/Ti-O-Cl drawn from Gibb's free energy data[19,20] is shown in Figure 2. The dotted lines indicate the phase boundaries between metal oxides and their chlorides at 10^{-3} atm (A-A′; TiO_2-$TiCl_4$ (0.001 atm), B-B′; SiO_2-$SiCl_4$ (0.001 atm)). The shaded area represents the range of conditions for producing iron chloride without chlorinating other oxides. When a range of 10^{-2} to 1 atm chlorine pressure is used in the practical chlorination, the partial pressure of oxygen must be controlled in the range 10^{-8} to 10^{-3} atm for the selective chlorination of iron. From Figure 2, the thermodynamic possibility to selectively chlorinate iron oxides without chlorinating titania and silica within this temperature range is seen. A similar analysis was previously discussed for the Al_2O_3/Fe_2O_3 system.[21]

In conjunction with this predominance area diagram, the results of chemical equilibrium calculations for the chlorination are shown in Figures 3 and 4 which were obtained from available computer software using the energy minimization method. Figure 3 illustrates the equilibria for gaseous and condensed phases, while Figure 4

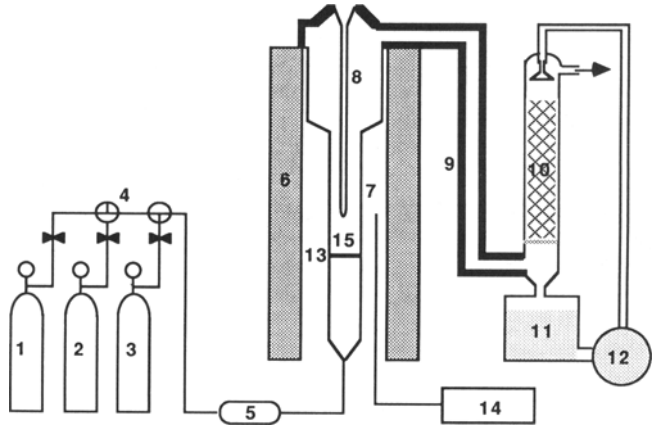

Fig. 1—Schematic diagram of the experimental apparatus for chlorination by CO/Cl_2 mixture. (1) chlorine cylinder, (2) carbon monoxide cylinder, (3) nitrogen cylinder, (4) gas control system, (5) rotameter, (6) furnace, (7) chlorinator, (8) thermocouple well, (9) heating tape, (10) packed column, (11) reservoir, (12) pump, (13) gas distributor, (14) temperature controller, and (15) sample.

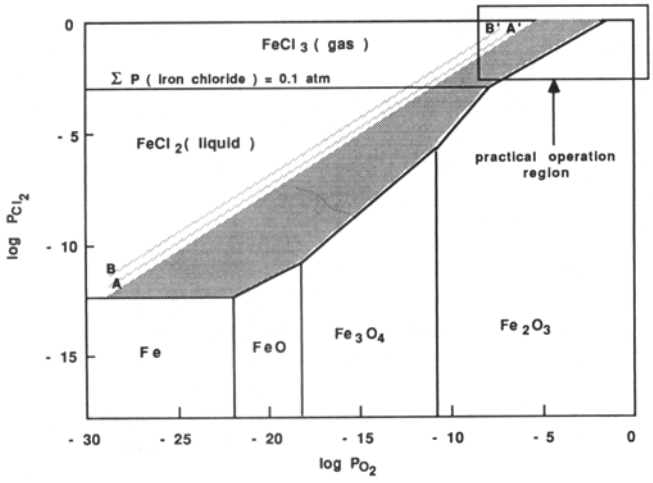

Fig. 2—Fe(Ti, Si)-Cl-O predominance area diagram at 973 K. Dotted lines A-A′ and B-B′ are the $TiCl_4$-TiO_2 and SiO_2-$SiCl_4$ phase boundaries, respectively, at 10^{-3} atm.

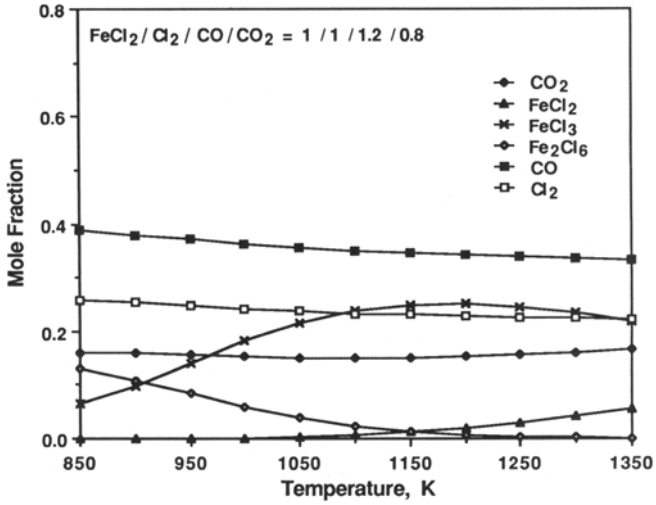

Fig. 4—Thermodynamic equilibria for the reaction of chlorine with the product gases from ilmenite chlorination.

presents that for only gaseous phases. These figures show that iron oxides are initially chlorinated to $FeCl_2$ which, in turn, is further chlorinated to $FeCl_3$ by Cl_2 in the gas phase.

The selective chlorination of iron was achieved over the range of conditions established, as shown by the results in Figure 5. The fractions of iron and titanium chlorinated were obtained from weight loss measurement and chemical analysis. The figure shows that the maximum loss of TiO_2 was less than 7 pct, while the removal of iron was as high as 94 pct. The major reactions in the selective chlorination of ilmenite ore are considered to be

$$FeTiO_3 + \frac{3}{2}Cl_2 + CO = FeCl_3 + TiO_2 + CO_2 \quad [1]$$

$$Fe_2O_3 + 3Cl_2 + 3CO = 2FeCl_3 + 3Cl_2 \quad [2]$$

B. *Effects of Variables*

1. *Effect of flow rate*

Richardson and Szekely[22] found that the elimination of mass- and heat-transfer effects at the low range of Reynolds numbers in a fluidized bed was usually difficult, but these effects can be removed without any elutriation of solids in a shallow bed using a higher flow rate. A series of experiments with respect to various space velocities was performed to determine whether the mass-transfer effect of gaseous reactants and products influenced reaction rate. Conversion rate increased with increasing flow rate but was essentially independent of flow rate beyond 600 cm^3/min (298 K and 86.1 kPa).[23] Based on this observation, a flow rate of 900 cm^3/min (298 K and 86.1 kPa), which is about 9 times higher than the minimum fluidization velocity, was used for subsequent experiments.

2. *Effect of particle size*

The experimental results of four different size fractions at two different temperatures of 923 and 1023 K are shown in Figure 6. This figure shows that the effect of particle size on the rate is not significant. Microscopic examination helped to explain this phenomenon; it revealed that a large number of pores were produced after

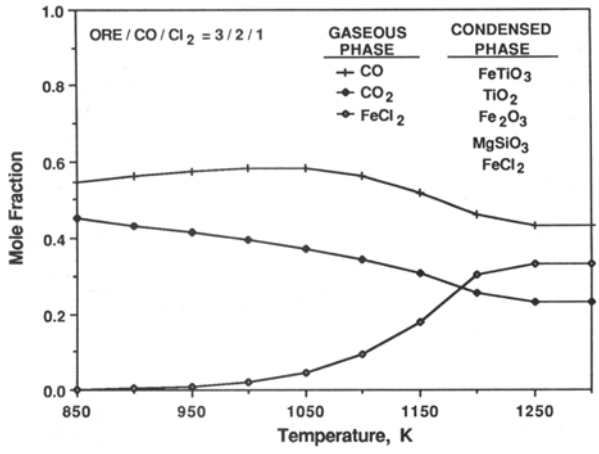

Fig. 3—Thermodynamic equilibria for the chlorination of ilmenite ore with carbon monoxide/chlorine gas mixture from the energy minimization calculation.

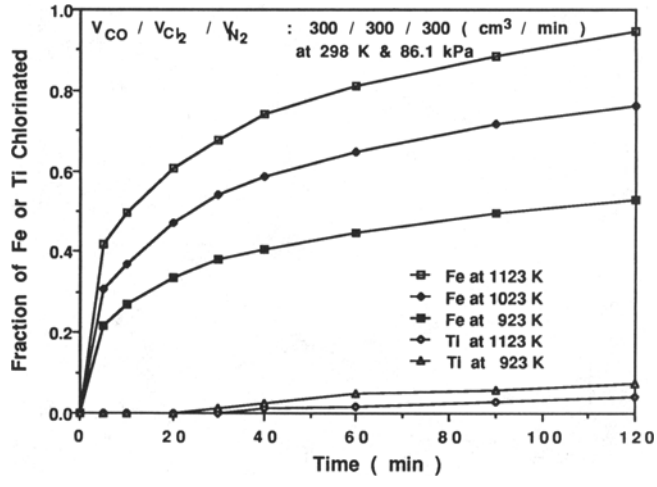

Fig. 5—Comparison of conversion *vs* time for iron and titanium chlorination from ilmenite ore with carbon monoxide (V = volumetric flow rate at 298 K and 86.1 kPa).

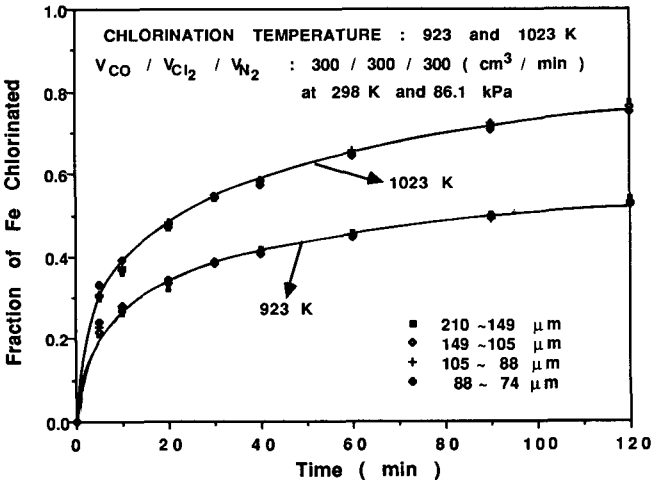

Fig. 6—Effect of particle size on the chlorination of ilmenite (V = volumetric flow rate at 298 K and 86.1 kPa).

a short period of reaction, and pore size increased with increasing conversion, as shown in Figures 7 and 8. The general tendency of smaller particles reacting faster is evident in the very early stages of reaction. However, as the reaction continues and the pores become larger, the dependency of the rate on particle size disappears, because these large pores provide easy access for reacting gases.

3. *Effect of carbon monoxide and chlorine partial pressure*

Experiments were conducted with various mixtures of CO and Cl_2 to investigate the effects of their partial pressures. The experimental results, together with the calculated lines obtained from the pore-blocking rate law described below, are compared in Figures 9 and 10. As these figures show, the rate of reaction is rapid during the short initial period and then slows down. After several rate expressions were tested to fit these experimental

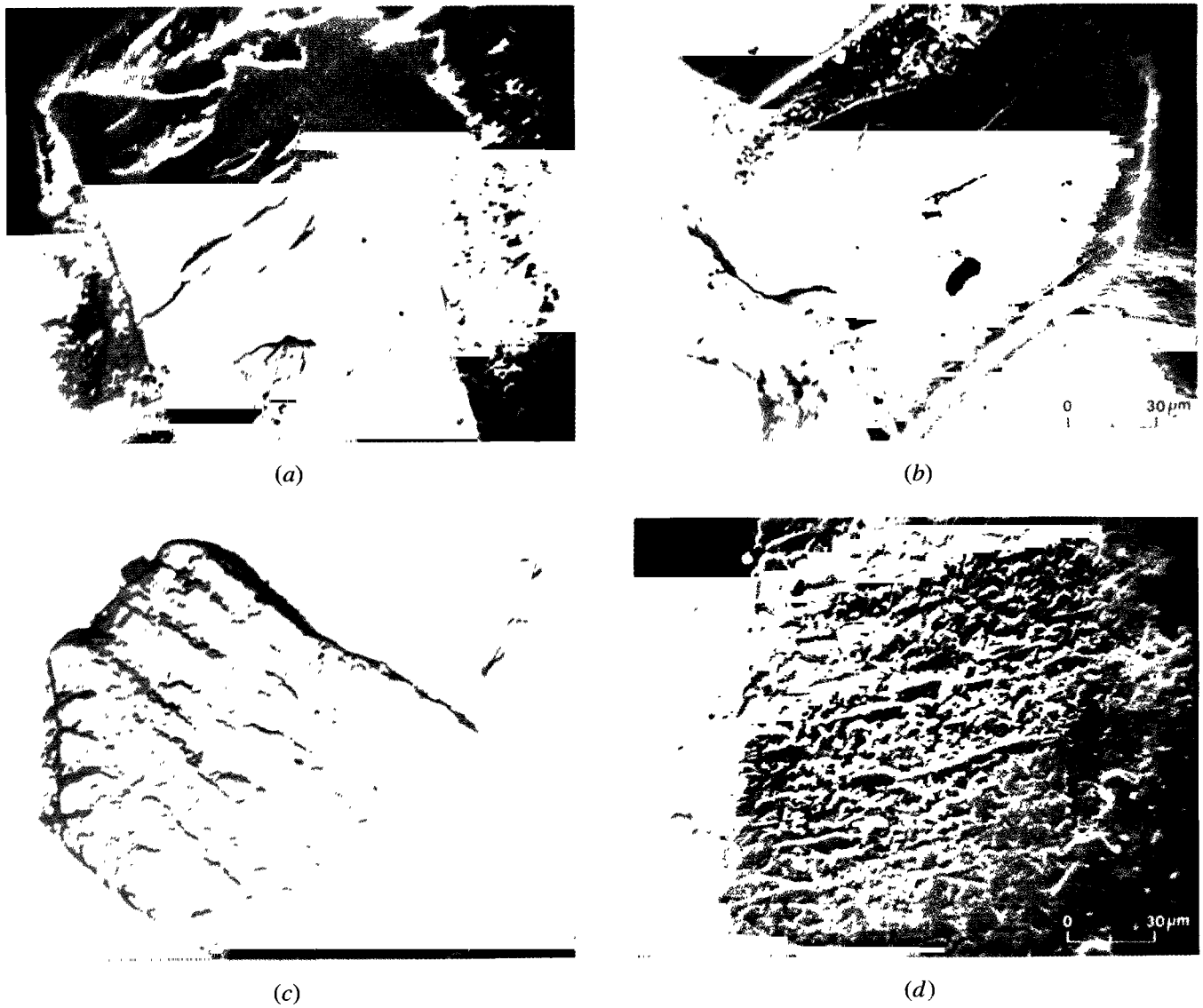

(*a*) (*b*) (*c*) (*d*)

Fig. 7—Micrographs of the cross section of particles: (*a*) original ore, (*b*) 21 pct conversion, (*c*) 53 pct conversion, and (*d*) 74 pct conversion.

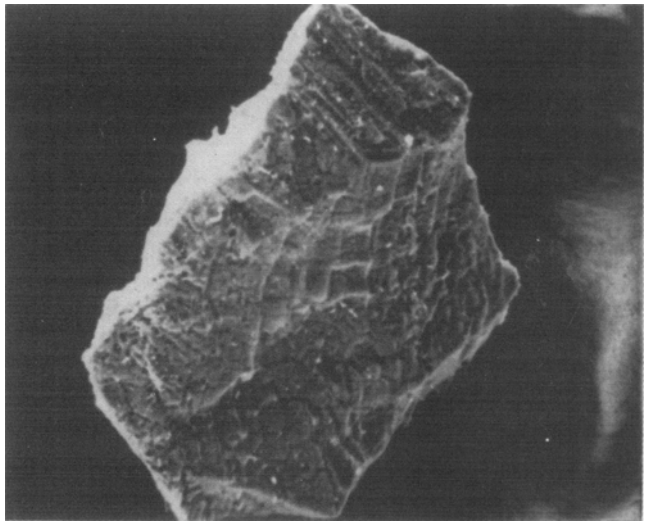

(*a*)

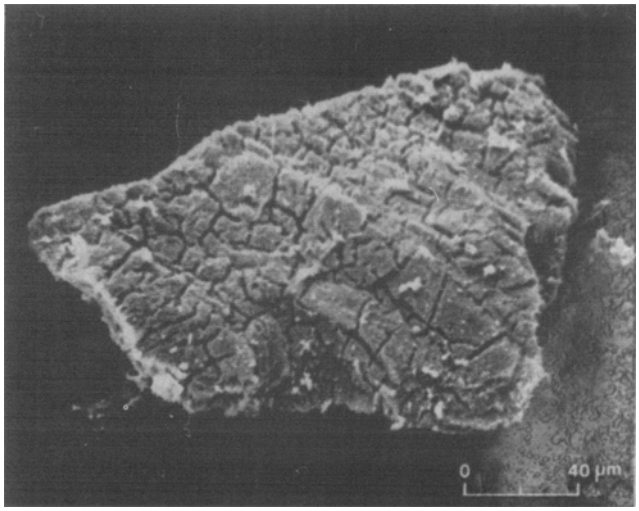

(*b*)

Fig. 8—Micrographs of entire particles of partially reacted ore: (*a*) 21 pct conversion and (*b*) 53 pct conversion.

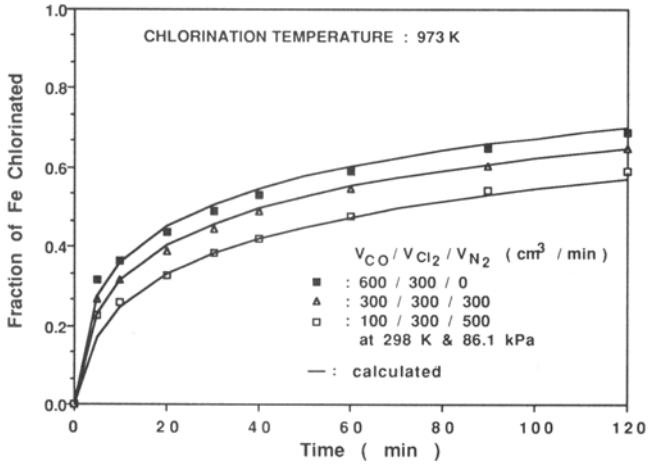

Fig. 9—Effect of the partial pressure of carbon monoxide on the chlorination (V = volumetric flow rate at 298 K and 86.1 kPa).

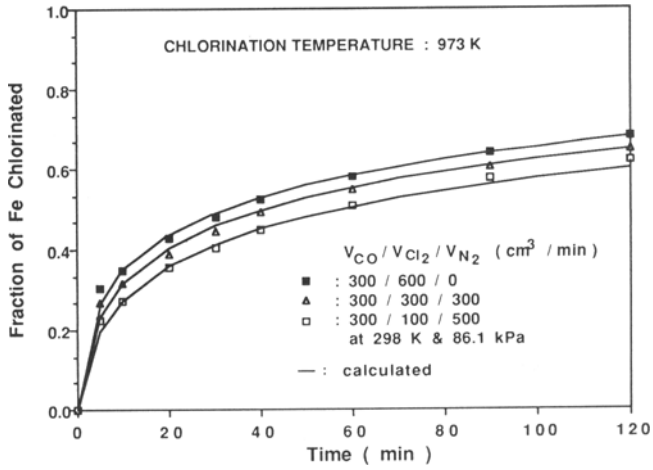

Fig. 10—Effect of the partial pressure of chlorine on the chlorination (V = volumetric flow rate at 298 K and 86.1 kPa).

data, the following pore-blocking rate law was found to give the most satisfactory correlation of these results:

$$k_a t = \lambda[\exp(X_{Fe}/\lambda) - 1] \quad [3]$$

where λ and k_a are constants with respect to conversion. The constant λ is related to pore blockage which inhibits the access of the reacting gases. This is likely to be due to the formation of high-boiling liquid phase intermediates. Although an in-depth examination of the pore-blocking phenomenon in this system was not made, it will be shown that this rate equation can adequately represent the chlorination rate.

The apparent rate constant, k_a, can be expressed as

$$k_a = kf(p_{CO}, p_{Cl_2}) \quad [4]$$

where k is the rate constant and $f(p_i)$ is a function of the partial pressure of gas species i.

According to Eq. [3], a correct value of λ will yield a straight line when the term on the right-hand side is plotted against time for each run. Examples of such plots are shown in Figures 11 and 12. The results of all other runs under different sets of pressures and temperatures produce similar straight lines, as shown in Figures 13 and 14. It is of interest to observe the constant value of

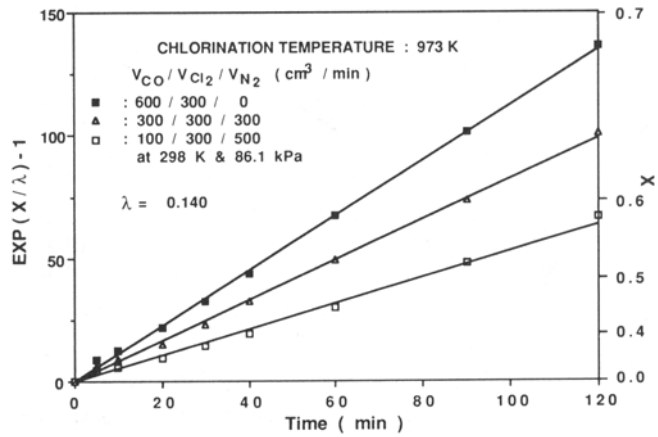

Fig. 11—Plot of exp (X/λ) − 1 *vs* time from Fig. 9.

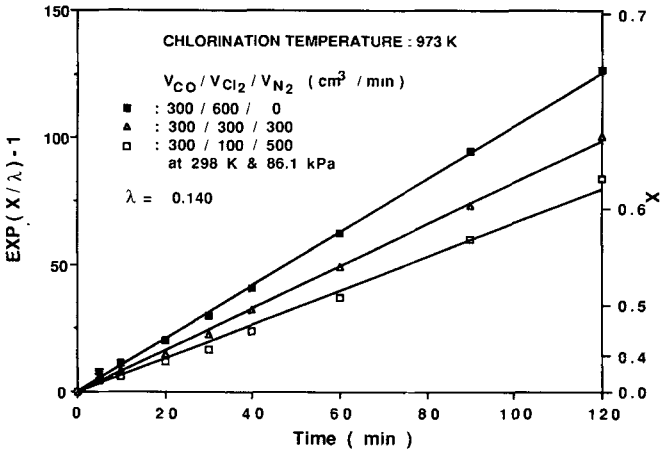

Fig. 12—Plot of exp $(X/\lambda) - 1$ *vs* time from Fig. 10.

λ in all the plots for various combinations of gas mixtures at constant temperature. Hence, the value of λ varies only with temperature and is independent of the partial pressure of CO and Cl_2 gases. Then, assuming that $f(p_{CO}, p_{Cl_2})$ takes the form of $p_{CO}{}^m p_{Cl_2}{}^n$, m and n were obtained from slopes in plots for different partial pressures of chlorine gas, holding the partial pressure of carbon monoxide gas constant and *vice versa* (Figure 15). These values at different temperatures are presented in Table III. Using average values representing the dependency of chlorination rate on partial pressures of CO and Cl_2, Eq. [3] can be rewritten as follows:

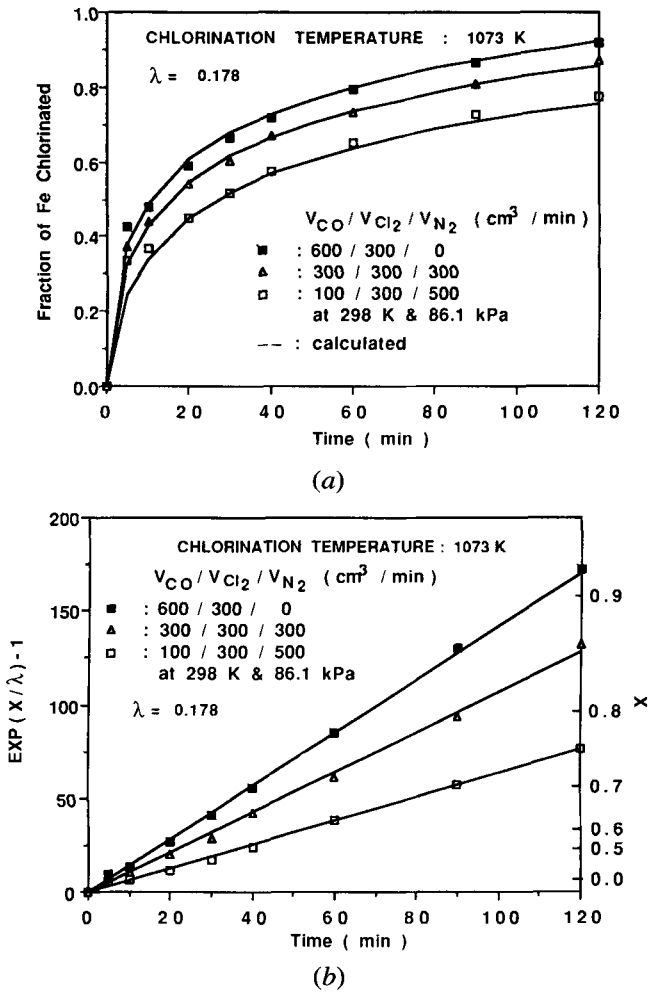

Fig. 13—(*a*) Effect of the partial pressure of carbon monoxide on the chlorination at 1073 K. (*b*) Plot of exp $(X/\lambda) - 1$ *vs* time from (a) (V = volumetric flow rate at 298 K and 86.1 kPa).

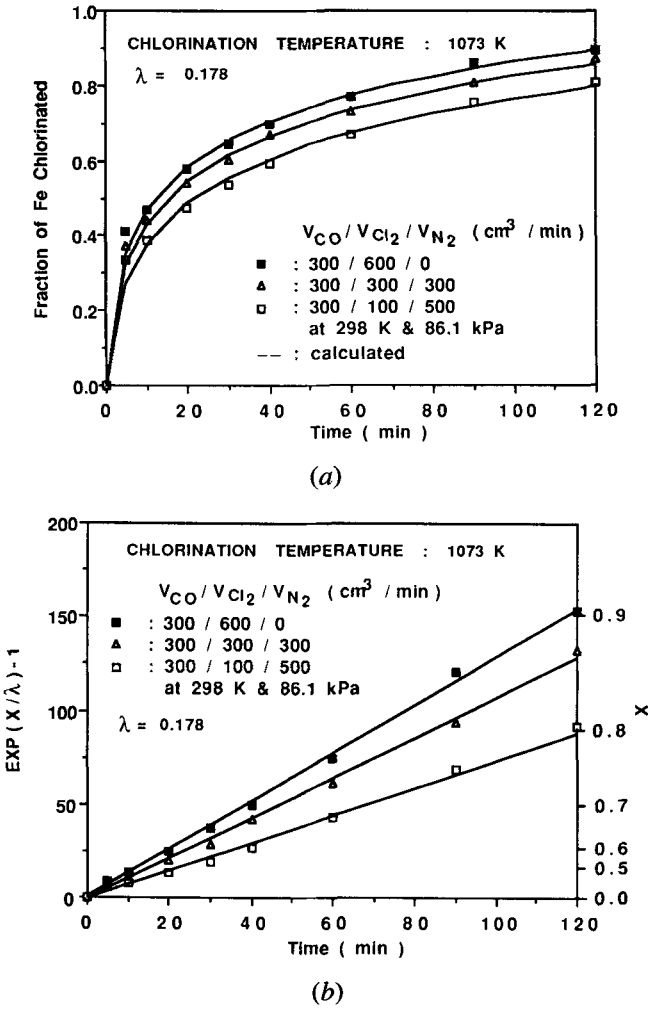

Fig. 14—(*a*) Effect of the partial pressure of chlorine on the chlorination at 1073 K. (*b*) Plot of exp $(X/\lambda) - 1$ *vs* time from (a) (V = volumetric flow rate at 298 K and 86.1 kPa).

$$\lambda\left[\exp\left(\frac{X_{Fe}}{\lambda}\right) - 1\right] = k p_{CO}^{0.52} p_{Cl_2}^{0.32} t \qquad [5]$$

The exponents in this equation confirm the experimental observation that the effect of CO partial pressure on the reaction rate is stronger than that of Cl_2 partial pressure.

4. *Effect of temperature*

To determine the effect of temperature on the reaction rate, experiments were carried out at different temperatures under constant partial pressures of CO and Cl_2. The results are shown in Figure 16, and the corresponding plot of conversion function *vs* time using appropriate values of λ gives straight lines, as shown in Figure 17. The rate constant, k, can be obtained from the slopes in Figure 17 and the use of Eq. [5]. Figure 18 shows an Arrhenius plot and the best-fit straight line through these

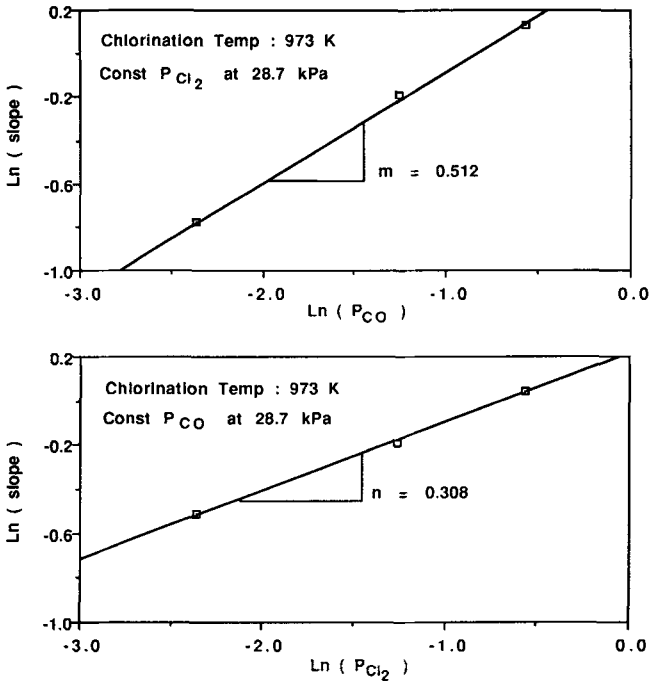

Fig. 15—Plots of ln (slope) *vs* ln p_{CO} and ln p_{Cl_2} obtained from Figs. 11 and 12.

data. Therefore, the overall rate expression for the experimental data may be represented by

$$\lambda\left[\exp\left(\frac{X_{Fe}}{\lambda}\right) - 1\right] = 33.7 \exp\left(-\frac{E}{RT}\right) p_{CO}^{0.52} p_{Cl_2}^{0.32} t \qquad [6]$$

where the activation energy, E, is 37.2 kJ/mol, and p and t are in atm (=101.3 kPa) and minutes, respectively.

As seen in Figure 19, the parameter λ depends on temperature according to an Arrhenius-type relationship:

$$1/\lambda = 3.56 \times 10^{-1} \exp(2.96 \times 10^3/T) \qquad [7]$$

5. *Effect of partial pressure of ferric chloride*

To investigate the effect of partial pressure of ferric chloride on the reaction rate, experiments were carried out in which vaporized ferric chloride was added to the reactant gases. As observed in Figure 20, ferric chloride enhances the chlorination rate. In addition, the experimental results are well fitted by the above rate law except that the value of λ increases with increasing pressure of ferric chloride. This relationship is shown in Figure 21.

Although further experiments with various partial pressures of ferric chloride will be needed for a systematic analysis of this effect, the correlation of λ with three

Table III. Reaction Order of Carbon Monoxide and Chlorine at Different Temperatures

Temperature, K	*m*	*n*
923	0.548	0.322
973	0.512	0.308
1073	0.490	0.327

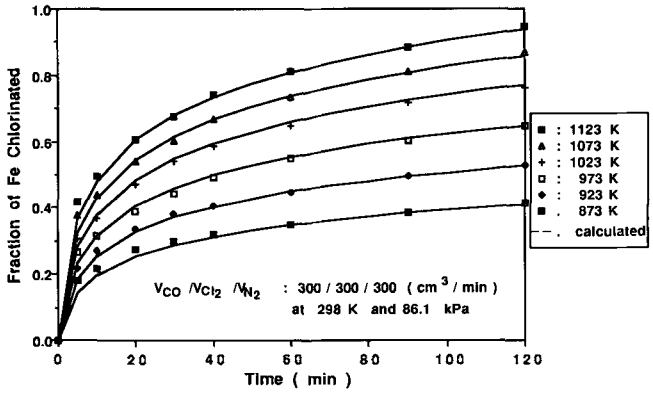

Fig. 16—Effect of temperature on the chlorination (V = volumetric flow rate at 298 K and 86.1 kPa).

different partial pressures of ferric chloride was obtained, as shown in Figure 22. The empirical relationship is

$$\lambda = \lambda_o(1 + 1.01\, p_{FeCl_3}^{0.62}) \qquad [8]$$

where $\lambda_o = 0.14$, and p_{FeCl_3} is in atm (=101.3 kPa).

The different dependency of the rate on $FeCl_3$ can be related to the changing reaction mechanism. Latina and Furman[24] studied the interaction mechanism of ferric chloride with ferric oxide. They found that at temperatures below 773 K, $FeCl_3$ partially combines with the ferric oxide to form iron oxychloride, and the thermal decomposition of FeOCl is completed above 773 K. In addition to this, it became evident that an unstable compound, $FeCl_3$-nFe_2O_3, of variable composition was formed at higher temperatures. Hence, they proposed that ferric chloride could be fully utilized to form unstable compound $FeCl_3$-nFe_2O_3 as a chlorinating agent above 773 K. Bezukladnikov and Pronichkin[25] found that the chlorination rate increased in the presence of iron chlorides and suggested the investigation of the mechanism and kinetics of chlorination of iron oxides by ferric chloride. Furthermore, Yu[26] discussed the catalytic influence of ferric chloride in the chlorination of ilmenite ore. While a detailed explanation for this behavior has not been given,

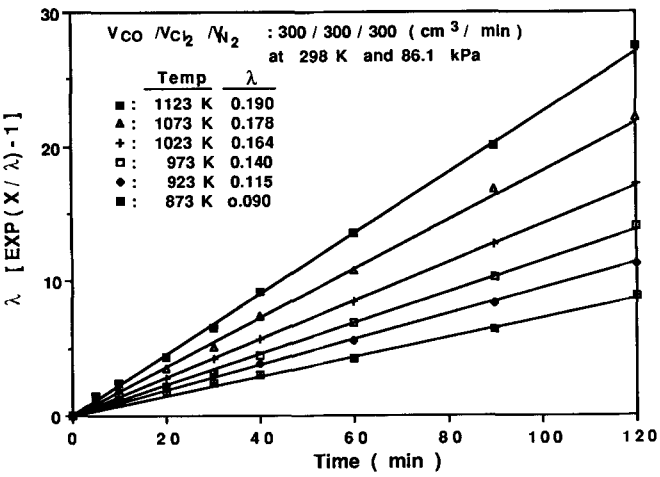

Fig. 17—Plot of $\lambda[\exp(X/\lambda) - 1]$ *vs* time from Fig. 16.

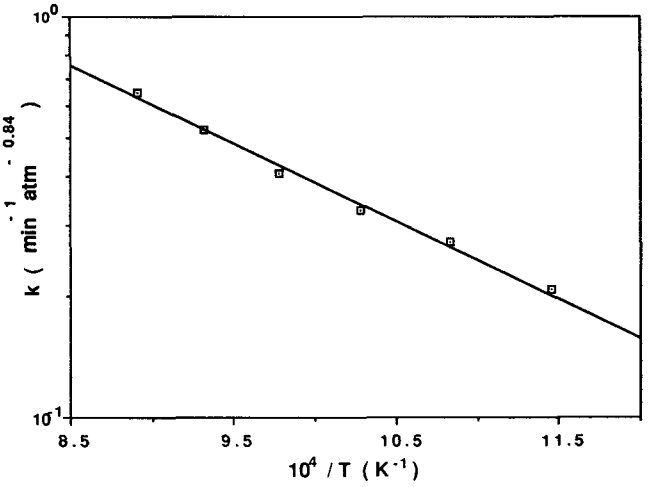

Fig. 18—Arrhenius plot of the rate constant for the chlorination.

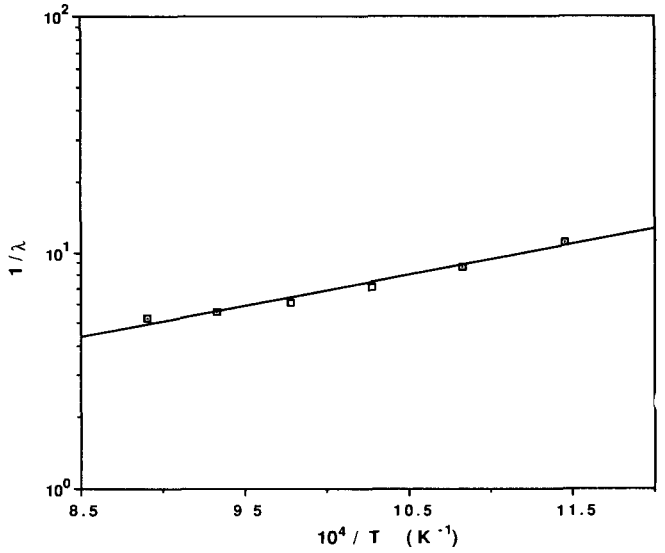

Fig. 19—Arrhenius-type plot of ln $(1/\lambda)$ *vs* $1/T$.

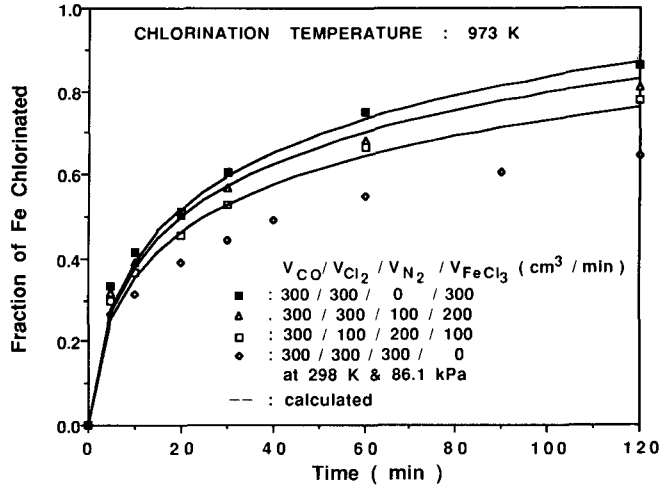

Fig. 20—Effect of the partial pressure of ferric chloride on the chlorination (V = volumetric flow rate at 298 K and 86.1 kPa).

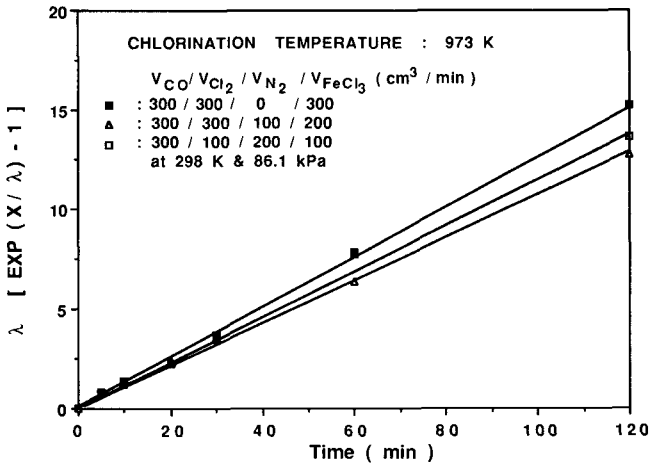

Fig. 21—Plot of $\lambda[\exp(X/\lambda) - 1]$ *vs* time from Fig. 20.

the iron oxide chlorination by ferric chloride can be described to proceed according to the following reaction:

$$Fe_2O_3 + 4FeCl_3 = 6FeCl_2 + \frac{3}{2}O_2 \qquad [9]$$

C. *Proposed Reaction Mechanism*

In order to determine the chlorination mechanism, experiments were carried out using only chlorine gas or carbon monoxide gas. Within the experimental range of temperatures (898 to 1123 K), carbon monoxide alone hardly reduced ilmenite;[27] however, as indicated by the initial sharp increase in conversion shown in Figure 23, chlorine gas alone reacted readily with the iron in ilmenite which is in the ferrous state. Furthermore, X-ray diffraction analyses of residue solid samples illustrated in Figure 24 confirmed that the ilmenite phase disappears after the short initial period of reaction, at which point the hematite phase becomes prevalent. Therefore,

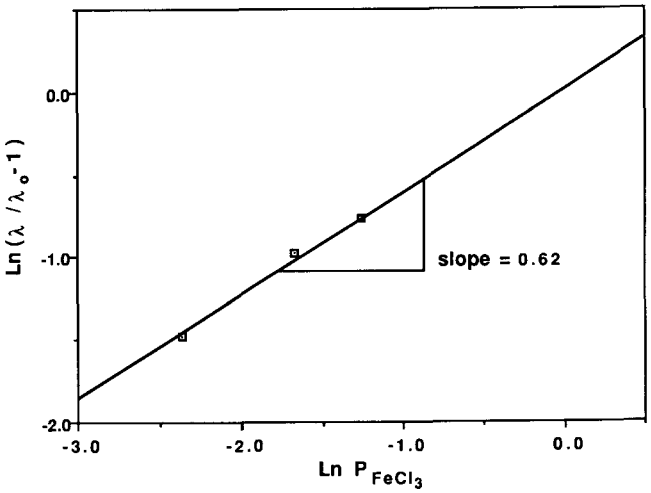

Fig. 22—Plot of ln $(\lambda/\lambda_o - 1)$ *vs* ln p_{FeCl_3}.

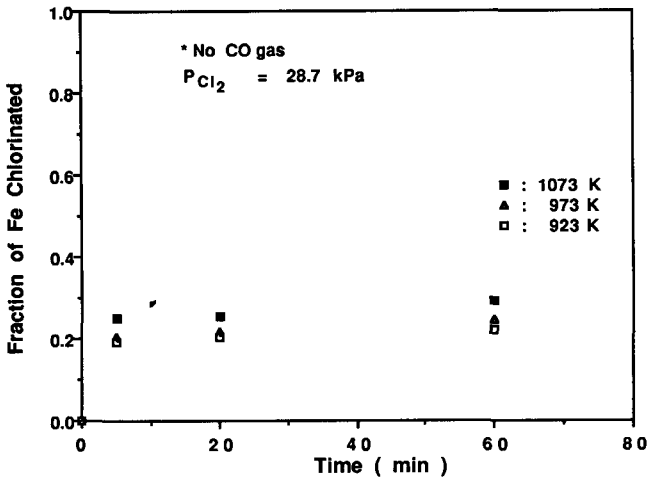

Fig. 23—Chlorination of ilmenite by chlorine gas alone without carbon monoxide at various temperatures.

although complicated reactions may be involved, the reaction mechanism for the selective chlorination, suggested by these experimental observations, can be presented as follows:

$$FeTiO_3 + Cl_2 + (FeCl_3) \rightarrow FeCl_2 + Fe_2O_3 + TiO_2 \quad [10]$$

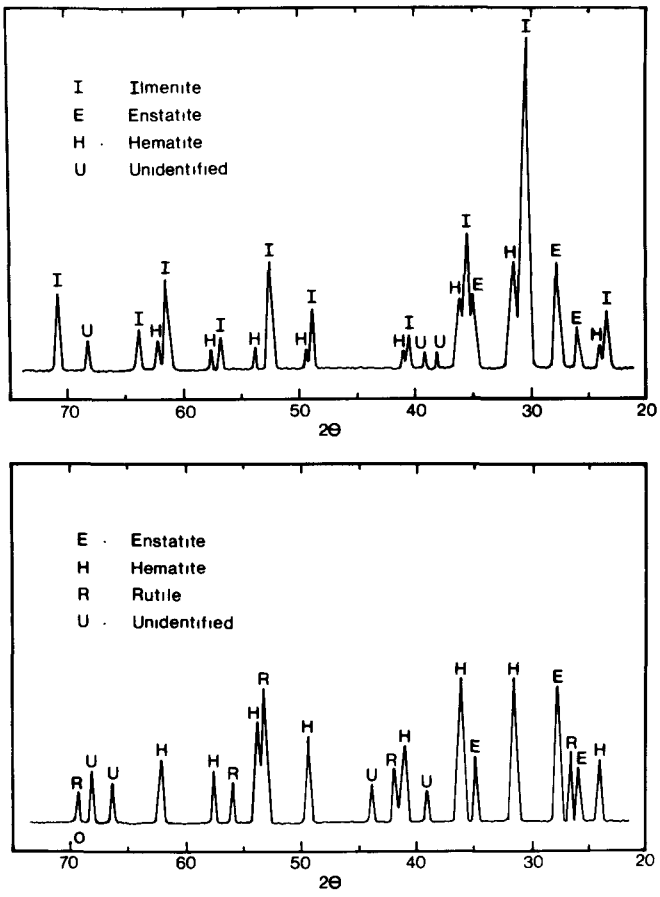

Fig. 24—Comparison of the X-ray diffraction pattern of original ilmenite ore (top) with that of solid residue from the chlorination by Cl_2 alone without CO gas at 973 K for 5 min (bottom).

$$Fe_2O_3 + Cl_2 + (FeCl_3) \rightarrow FeCl_2 + O_2 \quad [11]$$

$$FeCl_2 + \frac{1}{2}Cl_2 = FeCl_3 \quad [12]$$

$$O_2 + 2CO = 2CO_2 \quad [13]$$

The rates of Reactions [10] and [12] were experimentally confirmed to proceed fast, as mentioned above, and that of Reaction [13] is likely to take place fast in this temperature range. Consequently, the overall rate is considered to be controlled by Reaction [11]. The observed dependency of the overall rate on the partial pressure of chlorine is in good agreement with the thermogravimetric experimental result of Fuwa *et al.*[28] for the reaction of Fe_2O_3 in pseudobrookite with chlorine gas. This provides further support for the proposed mechanism.

IV. CONCLUSIONS

Through chlorination of iron in ilmenite ore in a very shallow fluidized bed reactor, the effects of various parameters on the chlorination rate were studied. The pore-blocking rate law was found to give the most satisfactory correlation of the experimental data. The effect of carbon monoxide partial pressure was greater than that of chlorine partial pressure. Furthermore, ferric chloride strongly enhances the chlorination rate, and the conversion increases with increasing partial pressure of ferric chloride. The chlorination rate did not depend on particle size.

Based on these observations, a reaction mechanism for the chlorination was proposed. The iron in ilmenite ore reacts with chlorine first, and then the liberated oxygen is removed by carbon monoxide.

ACKNOWLEDGMENTS

The authors wish to thank Drs. S.J. Im and D. Kim, both formerly with the Korea Institute of Energy and Resources, Daejeon, and now with Lucky Metals Corporation, Seoul, Korea, for many helpful discussions during the course of this work. This work was supported, in part, by the Department of the Interior's Mineral Institutes Program administered by the Bureau of Mines under Allotment Grant Nos. G1124149, G1134149, and G1144149 and by the National Science Foundation under Grant No. INT 82-11631.

REFERENCES

1. J.B. Rosenbaum: *Light Met.*, 1982, pp. 1123-34.
2. N.H. Orr: *Light Met.*, 1982, pp. 1149-56.
3. R. Powell: *Titanium Oxide and Titanium Tetrachloride*, Noyes Development Co., Park Ridge, NJ, 1968, pp. 1-6.
4. J. Barksdale: *Titanium: Its Occurrence, Chemistry, and Technology*, Ronald Press Co., New York, NY, 1966, pp. 10-46 and 213-23.
5. H.M. Harris, A.W. Henderson, and T.T. Campbell: U.S. Bureau of Mines, R.I. 8165, 1976, 19 pp.
6. L.K. Doraiswamy, H.C. Bijawat, and M.V. Kunte: *Chem. Eng. Prog.*, 1959, vol. 55 (10), pp. 80-88.

7. B.P. Judd and E.R. Palmer: *Proc. Australas. Inst. Min. Metall.*, 1973, vol. 247, pp. 23-33.
8. M.H. Tikkanan, T. Tyynela, and E. Vuoristo: *Metall. Soc. Conf.*, [Proc.] 1964, vol. 24, pp. 269-82.
9. G.W. Elger, J.B. Wright, J.E. Tress, H.E. Bell, and R.R. Jordan: U.S. Bureau of Mines, R.I. 9002, 1986, 24 pp.
10. G.W. Elger and W.A. Stickney: U.S. Bureau of Mines, Technical Progress Report-37, 1971, 9 pp.
11. C.D. Shiah: U.S. Patent No. 3,252,787, 1966.
12. S. Yamada: *Ind. Miner.*, 1976, vol. 1, pp. 33-40.
13. V.G. Neurgaonkar, A.N. Gorkan, and K. Joseph: *J. Chem. Technol. Biotechnol.*, 1986, vol. 36, pp. 27-30.
14. C.M. Lakeshmanan, H.E. Moelescher, and B. Chennakesavan: *Chem. Eng. Sci.*, 1968, vol. 20, pp. 1107-13.
15. A.S. Athavale and V.A. Altekar: *Ind. Eng. Chem. Process Des. Dev.*, 1971, vol. 10 (4), pp. 523-30.
16. K.I. Rhee and H.Y. Sohn: *Metall. Trans. B*, 1990, vol. 21B, pp. 331-40.
17. K.I. Rhee and H.Y. Sohn: *Metall. Trans. B*, 1990, vol. 21B, pp. 341-47.
18. I.M. Kolthoff, E.B. Sandell, E.J. Meehan, and S. Bruckenstein: *Quantitative Chemical Analysis*, 4th ed., 1969, pp. 752-53 and 838.
19. R.A. Robie, B.S. Hemingway, and J.R. Fisher: U.S. Geological Survey Bulletin 1452, 1979.
20. L.B. Pankratz, J.M. Stuve, and N.A. Gokcen: Bureau of Mines Bulletin 677, 1984, pp. 145-78.
21. D.J. Milne and R.D. Holliday: *Ind. Eng. Chem. Process Des. Dev.*, 1975, vol. 14 (4), pp. 442-52.
22. J.F. Richardson and J. Szekely: *Trans. Inst. Chem. Eng.*, 1961, vol. 39, pp. 212-21.
23. K.I. Rhee: Ph.D. Dissertation, University of Utah, Salt Lake City, UT, 1988.
24. Z.I. Latina and A.A. Furman: *Zh. Prikl. Khim.*, 1970, vol. 43 (4), pp. 830-34.
25. A.B. Bezukladninov and V.A. Pronichkin: *Zh. Prikl. Khim.*, 1972, vol. 45 (6), pp. 1221-24.
26. B. Yu: *Acta Metall. Sin.*, 1982, vol. 18 (2), pp. 164-75.
27. D.G. James: *Trans. Inst. Min. Metall.*, 1973, vol. 82, pp. C186-C192.
28. A. Fuwa, E. Kimura, and S. Fukushima: *J. Jpn. Inst. Met.*, 1980, vol. 44 (8), pp. 839-45.